

Light-induced structural changes by excitation of metastable states in $\text{Na}_2[\text{Fe}(\text{CN})_5\text{NO}]2\text{H}_2\text{O}$ single crystals

D. Schaniel* and J. Schefer

Laboratory for Neutron Scattering, ETHZ & PSI, CH-5232 Villigen, PSI, Switzerland

M. Imlau

Fachbereich Physik, University of Osnabrück, D-49069 Osnabrück, Germany

Th. Woike

Institut für Mineralogie, University at Cologne, D-50674 Köln, Germany

(Received 13 December 2002; revised manuscript received 5 March 2003; published 22 September 2003)

The structures of the ground state and the light-induced metastable state SI of $\text{Na}_2[\text{Fe}(\text{CN})_5\text{NO}]2\text{H}_2\text{O}$ were investigated by single-crystal neutron diffraction. We propose that a small but significant change in the Fe-N bond length ($\approx 0.05\text{\AA}$) and in the C-Fe-N angle ($\approx 3.5^\circ$) are the only rearrangements in the structure connected with the excitation of the metastable state SI. This result is consistently found for two data sets with different populations (22% and 44%) of the metastable state SI.

DOI: 10.1103/PhysRevB.68.104108

PACS number(s): 61.12.Ld, 33.15.Dj

I. INTRODUCTION

Any material possessing long-living metastable states, which can be reversibly transformed into each other by light, can be used as an information storage device or as fast optical switches. The photorefractive effect in such materials is based on a local molecular effect, and therefore the information is localized in the dimensions of molecules so that the storage capacity is extremely high.^{1,2}

Such light-induced metastable states can be excited in complexes containing the nitrosyl-ligand NO such as $[\text{ML}_x(\text{NO})]^n$, M being a transition metal, e.g., Fe, Ni, Ru, Os, and Mo, and n being the formal charge of the complex. The ligands L_x vary from atoms (F, Cl, Br, J, etc.) to complex ligands (CN, NH_3 , NO_2 , etc.).³⁻⁷ Compounds containing N_2 instead of NO as the active ligand were found recently,⁸ showing that these metastable states are based on a common physical effect.

$\text{Na}_2[\text{Fe}(\text{CN})_5\text{NO}]2\text{H}_2\text{O}$ (SNP, disodiumpentacyanonitrosylferrate) is the most investigated system in this class of compounds.^{9,10} In SNP two extremely long-living metastable states SI and SII can be excited below temperatures of about 198 K and 147 K, respectively. These states are separated from the ground state (GS) by potential barriers of 0.7 eV (SI) and 0.5 eV (SII), as determined from differential scanning calorimetry measurements.¹¹ They can be excited by irradiation with light in the spectral range of 350 to 580 nm. A maximum of about 50% of the $[\text{Fe}(\text{CN})_5\text{NO}]^{2-}$ molecules can be transferred into SI using light of wavelengths 440–470 nm polarized perpendicular to the quasifourfold N-C-Fe-N-O axis of the molecule. Relaxation into the ground state takes place either by illumination with light in the spectral range of 600–1200 nm or by increasing the temperature to overcome the potential barriers. Illumination with light in the region of 900–1200 nm below 147 K transfers about 30–35% of the molecules from SI into SII and the rest into the ground state.¹² Irradiation with light excites the elec-

trons from the GS into the antibonding $\pi^*(\text{NO})$ orbital. These excited electrons relax into the minimum of the $\pi^*(\text{NO})$ potential. At the crossing point of the potentials of GS and SI the relaxation back into GS or into SI occurs together with the thermalization process, since no luminescence is observed in the spectral range of 300 to 3000 nm. The high potential barriers of 0.7 eV (SI) and of 0.5 eV (SII) cause the stability of SI/SII at sufficiently low temperatures. The irradiation of SI in the range of 600–1200 nm leads again to the excitation of the $\pi^*(\text{NO})$ orbital, from which a relaxation into GS or into SII occurs. The four-level system GS, $\pi^*(\text{NO})$, SI, SII (Fig. 1) describes the population, depopulation, and transfer between GS, SI, and SII completely.¹³ The new states SI, SII are lying energetically about 1 eV above the ground state.¹²

The structure of the ground state of SNP is well known since its first determination by Manoharan and Hamilton¹⁴ and the subsequent redetermination by Bottomley and White.¹⁵ The first attempt to determine the structure of the metastable state SI was done with neutron diffraction,¹⁶ whereby an elongation of the Fe-N [$0.019(2)\text{\AA}$] and N-O

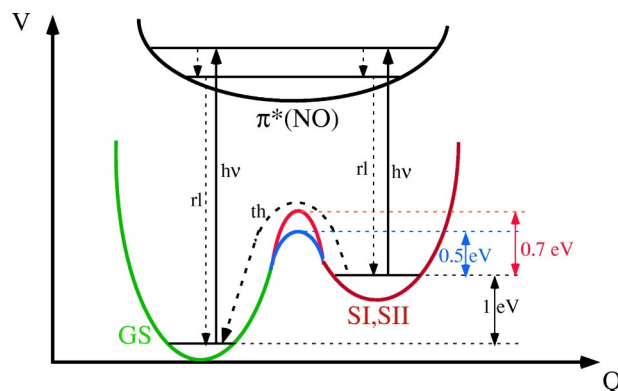


FIG. 1. Schematic drawing of the potential V for the four-level system GS, $\pi^*(\text{NO})$, SI, SII in SNP as a function of the reaction coordinate Q (rl: radiationless transition; th: thermal excitation).

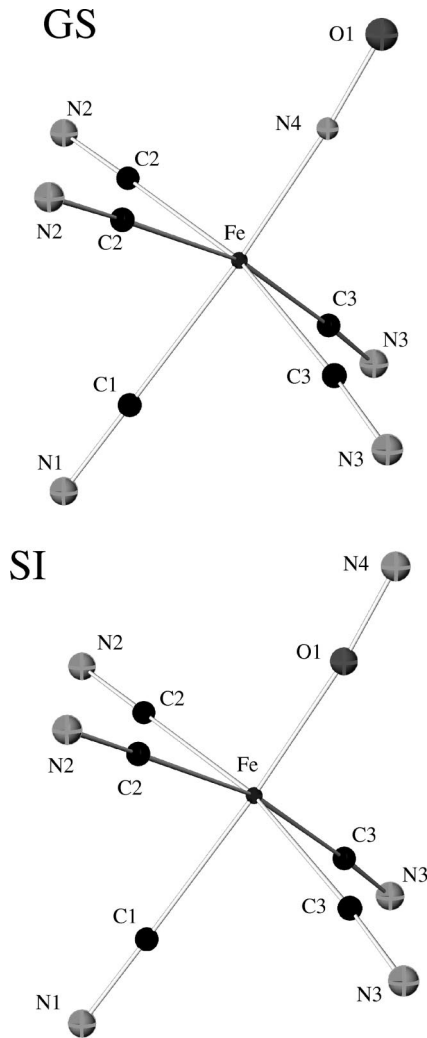


FIG. 2. GS and isonitrosyl (SI) configuration of the $[\text{Fe}(\text{CN})_5\text{NO}]^{2-}$ molecule in SNP, as proposed by Carducci *et al.*¹⁷ View along the c axis (10° inclined).

[$0.004(4)$ Å] bond lengths compared to the ground state was found. Subsequent x-ray studies confirmed this result.^{17,18} From their x-ray study Pressprich *et al.*¹⁸ concluded that the Fe-N bond is elongated by $0.049(8)$ Å from $1.668(1)$ Å in the ground state to $1.717(8)$ Å in SI, and that the *cis* angles N-Fe-C are decreased from $95.51(3)^\circ$ to $94.75(19)^\circ$. Carducci *et al.*¹⁷ confirmed these results [lengthening of the Fe-N distance by $0.053(6)$ Å and increase of C2-Fe-C3 angle by 1.1°]. However, the authors of the latter article suggest another structural configuration for SI: an isonitrosyl configuration Fe-O-N (see Fig. 2) yields the same agreement factors in the refinement as for the nitrosyl configuration Fe-N-O. Calculations using density-functional theory¹⁹ (DFT) showed that the isonitrosyl configuration provides indeed a local minimum in energy. Nevertheless, in a reexamination of the neutron results¹⁵ the isonitrosyl configuration for SI failed to explain the experimental data. In all the above-mentioned experiments the determination of the population of SI, i.e., the number of $[\text{Fe}(\text{CN})_5\text{NO}]^{2-}$ molecules which are excited into the metastable state, is somewhat cumbersome.

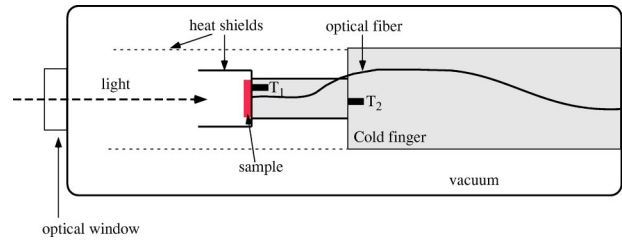


FIG. 3. Schematic drawing of the cooling device equipped with an optical window and fiber optics in order to illuminate the sample and to measure the transmitted light intensity. T_1 and T_2 are temperature sensors.

In order to clarify the structure of the metastable state SI, we performed neutron diffraction experiments on single crystals of deuterated SNP. The population of SI was independently determined by a transmission measurement. As shown in a previous paper²⁰ the change in transmitted light intensity can be used to determine the population of SI in SNP accurately. Thereby neither assumptions about the correlation between the change in the lattice parameters and the population of SI nor extrapolations from other experimental techniques via the illumination time have to be made.

II. EXPERIMENT

The neutron-diffraction experiments were performed on the single-crystal diffractometer TriCS (Ref. 21) at the Swiss Spallation Source SINQ (Ref. 22) at PSI/Villigen using a single detector. The SNP samples were mounted on a sample holder as indicated in Fig. 3 in a closed cycle refrigerator. The refrigerator is equipped with an optical window (quartz) to allow for the illumination of the sample with polarized light down to temperatures of 10 K. In order to guarantee thermal stability at low temperature additional heat shields (aluminum) were mounted. The temperature was measured with two sensors. The temperature sensor T_1 was placed directly behind the sample position, as indicated in Fig. 3. The second sensor T_2 was placed on the cold finger and was used to control the temperature (see Fig. 3). A deuterated single crystal of SNP (diameter 9 mm, thickness $d=0.9$ mm) was used. First the mixed state GS+SI was excited by illuminating the crystal with laser light of wavelength 476.5 nm and polarization along the c axis of the crystal. The average intensity was 100 mW/cm^2 so that after 100 h of illumination time a total exposure $Q \approx 36\,000 \text{ Ws/cm}^2$ was achieved. After the measurement of a full dataset at 43 K (sensor T_1) of the excited state (1134 reflections) the crystal was heated to 200 K in order to depopulate SI. Afterwards the same dataset was measured in the GS at 43 K (sensor T_1). The temperature at the sensor T_2 was stabilized at 30 K.

The population P_{SI} of the metastable state SI during the neutron-scattering experiment can be determined by measuring the transmitted light intensity behind the SNP crystal. Therefore a fiber optic was introduced in the refrigerator guiding the light to a photodiode, which is stable at room temperature. The voltage over the diode is proportional to the transmitted light intensity. An amplifier with selectable load resistors guarantees a linear behavior in intensity over many

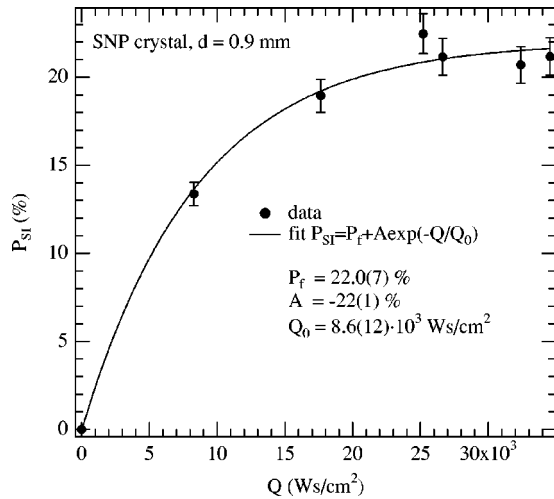


FIG. 4. Population as a function of exposure Q of a SNP crystal ($d=0.9$ mm). The polarization of the light was along the c axis of the crystal and therefore perpendicular to the N-C-Fe-N-O axis. A wavelength of 476.5 nm of an Ar^+ laser with an average power of 100 mW/cm^2 was used. A final population of $P_f=22\%$ is reached with this setup.

decades. Figure 4 shows the population measured on a SNP crystal of thickness $d=0.9$ mm, which was illuminated with laser light of the wavelength 476.5 nm and an average power of 100 mW/cm^2 . The temperature during the illumination was 46 K, as monitored by sensor T_1 . The measured voltage U_{ph} is proportional to the transmitted light intensity I_t given by the incident light intensity I_0 of the laser beam and the damping in the sample:

$$U_{ph} \sim I_t = I_0 \exp(-\alpha d), \quad (1)$$

where α is the absorption coefficient of the sample and d is the thickness of the sample. Measuring the transmitted light intensity one can therefore determine the absorption coefficient α of the crystal in the mixed state GS+SI by

$$\alpha_{\text{GS+SI}}(Q) = \alpha_{\text{GS}}(Q=0) - \frac{1}{d} \ln \left(\frac{I_{t,\text{GS+SI}}}{I_{t,\text{GS}}} \right). \quad (2)$$

The absorption coefficients of GS and the mixed states GS+SI are precisely known from absorption measurements, as demonstrated in detail in Ref. 20. Therefore the population P_{SI} of the metastable state SI can be determined by comparing $\alpha_{\text{GS+SI}}(Q)$ and $\alpha_{\text{GS}}(0)$ at the corresponding wavelength (476.5 nm) using Eq. (6) from Ref. 20:

$$P_{\text{SI}}(Q) = \frac{\alpha_{\text{GS}}(Q=0) - \alpha_{\text{GS}}(Q)}{\alpha_{\text{GS}}(Q=0)}. \quad (3)$$

The knowledge of the actual population P_{SI} of the metastable state SI is of great importance for the refinement of the structure. Therefore in a further neutron-diffraction experiment on the two-axis spectrometer TOPSI at SINQ the neutron structure factor of selected reflections was recorded as a function of the population P_{SI} of SI, which was determined from the transmission measurement using the setup shown in

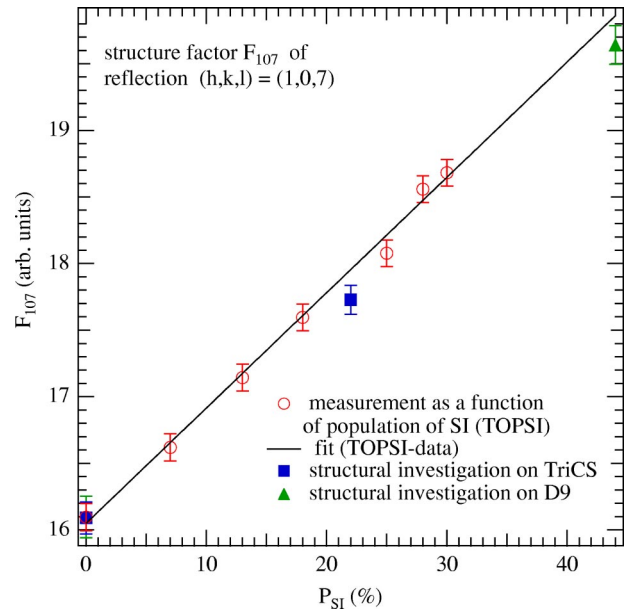


FIG. 5. Structure factor F_{107} as a function of the population of SI (P_{SI}) of a SNP crystal ($d=0.85$ mm). The polarization of the light was along the c axis of the crystal. A wavelength of 476.5 nm of an Ar^+ laser with an average power of 50 mW/cm^2 was used. The structure factors F_{107} obtained in the two experiments on TriCS and D9 are indicated for comparison.

Fig. 3. Figure 5 shows the structure factor F_{107} as a function of P_{SI} . It shows a linear dependence on P_{SI} , since the phases are 0 or π in the centrosymmetric space group $Pn\bar{1}m$ ($F_{107} = \sqrt{I_{107}}$, I_{107} : scattered-neutron intensity). The reflection 107 proves to be useful for a comparison between the different crystals used in the different measurements, since it is a weak reflection and therefore does not suffer from changes in the extinction, which occur when illuminating the crystal with laser light. The values of the structure factor F_{107} obtained in the two structural investigations on TriCS at SINQ and on D9 at ILL (Ref. 17) are indicated in Fig. 5. The values of the different measurements have been scaled to the ground-state value of F_{107} . Figure 5 illustrates that the populations P_{SI} of SI assumed for the refinement of the two datasets agree very well with the TOPSI results. Therefore in future experiments one may also check the achieved population P_{SI} of SI by comparing the structure factor F_{107} with this curve.

III. REFINEMENT

The structural refinement of the neutron data of GS and the mixed state GS+SI is performed with the program JANA2000. (Ref. 23) For both states the space group $Pn\bar{1}m$ (No. 58) is used. The lattice parameters $a=6.1663(6) \text{ \AA}$, $b=11.8904(8) \text{ \AA}$, and $c=15.6003(17) \text{ \AA}$ for GS and $a=6.1357(3) \text{ \AA}$, $b=11.8545(7) \text{ \AA}$, and $c=15.5461(10) \text{ \AA}$ for GS+SI were refined from 820 observed reflections using the program Refin/ILL. The neutron wavelength was $1.1761(13) \text{ \AA}$ as was determined after the measurement with a NaCl single crystal with $a=6.6400(5) \text{ \AA}$.²⁴ Isotropic extinction correction of type I (Lorentz distribution) is

TABLE I. Experimental data collection parameters for SNP.

	GS (TriCS)	GS+SI (TriCS)	GS (D9)	GS+SI (D9)
Space group	<i>Pnmm</i>	<i>Pnmm</i>	<i>Pnmm</i>	<i>Pnmm</i>
Z	4	4	4	4
Wavelength λ (Å)	1.1761(13)	1.1761(13)	0.8489(4)	0.8489(4)
T(K)	43	43	80	80
<i>a</i> (Å)	6.1663(6)	6.1357(3)	6.1679(5)	6.1818(5)
<i>b</i> (Å)	11.8904(8)	11.8545(7)	11.9033(10)	11.9182(8)
<i>c</i> (Å)	15.6003(10)	15.5461(10)	15.6124(13)	15.6198(11)
<i>V</i> (Å ³)	1143.8	1130.8	1146.2	1150.8
<i>d</i> (g/cm ³)	1.728	1.736	1.757	1.757
$[\sin(\theta)/\lambda]_{\max}$ (Å ⁻¹)	0.706	0.706	0.732	0.729
Absorption coefficient (mm ⁻¹)	0.004	0.004	0.003	0.003
<i>T</i> _{min} (minimum transmission)	0.9721	0.9709	0.9849	0.9845
<i>T</i> _{max} (maximum transmission)	0.9952	0.9951	0.9973	0.9973
Crystal dimension (mm ³)	0.9·4.5·4.5 ^a	0.9·4.5·4.5 ^a	0.3·3·3	0.3·3·3
<i>h</i> _{max}	7	7	8	8
<i>k</i> _{max}	14	14	15	17
<i>l</i> _{max}	18	18	20	22
No. of measured reflections	1134	1134	1567	2111
No. of unique reflections	951	951	1401	1837
Merging <i>R</i> _{e.s.d.}	0.0108	0.0109	0.0312	0.0219
Merging <i>R</i> _{int}	0.0135	0.0116	0.0191	0.0327
No. of refined reflections	1015	1015	1567	2111
No. of observed reflections (<i>I</i> > 3σ)	908	964	1401	1837
<i>g</i> _{iso} ^b (10 ⁻⁴)	0.001 258	0.001 191	0.001 490	0.003 201
Population of SI <i>P</i> _{SI} (%)	0	22	0	44

^aCircular sample of diameter 9 mm.

^bIsotropic extinction correction of type I (Lorentzian distribution) is used (Ref. 23).

applied.²⁵ 1015 reflections (908 observed) are considered for the refinement of GS and 1015 (964) for the mixed state GS+SI.

In order to check the reliability of the refinement and the chosen models, the datasets for GS and GS+SI, measured by Rüdinger *et al.*¹⁶ at the single-crystal diffractometer D9 at ILL (*T*=80 K), have been reexamined with JANA2000, as this program package offers more options for complicated restrictions than the program UPALS (Ref. 26) used in the former study. The lattice parameters for the two D9 datasets are *a*=6.1679(5) Å, *b*=11.9033(10) Å, and *c*=15.6124(13) Å for GS and *a*=6.1818(5) Å, *b*=11.9182(8) Å, and *c*=15.6198(11) Å for GS+SI. The neutron wavelength in this experiment was 0.8489(4) Å. 1567 reflections (1402 observed) are considered for the refinement of GS and 2111 (1838) for the mixed state GS+SI. The lattice parameters for the crystal used in the D9 experiment were redetermined from the positions of 1000 observed reflections. Therefore they differ slightly from those given in Ref. 16, which are based on a set of 20 reflections.

The refinement is based on the nuclear structure factor

$$F(\mathbf{Q}) = \sum_j b_j \exp(i\mathbf{Q}\mathbf{R}_j) \exp[-W_j(\mathbf{Q})], \quad (4)$$

where *b_j* denotes the neutron-scattering length,²⁷ \mathbf{R}_j is the position of atom *j*, and \mathbf{Q} is the momentum transfer. The sum has to be performed over all atoms *j* in the unit cell and *W_j* is the Debye-Waller factor.

The quality of the refinement is described by the agreement factors *R* and *goodness of fit S*. The *R* factor is defined as

$$R = \frac{\sum_{hkl} ||F_{\text{obs}}| - |F_{\text{calc}}||}{\sum_{hkl} |F_{\text{obs}}|}, \quad (5)$$

where *F*_{obs,calc} are the observed and calculated structure factors. Goodness of fit *S* is defined as

$$S = \sqrt{\frac{\sum w(F_{\text{obs}} - F_{\text{calc}})^2}{m - n}}, \quad (6)$$

where *m* is the number of reflections and *n* is the number of parameters refined. The weight *w* is defined as

$$w = \frac{1}{\sigma^2(|F_{\text{obs}}|) + (uF_{\text{obs}})^2}, \quad (7)$$

where σ is the observed standard deviation of the structure factor and u is the instability factor ($u=0.01$ in our refinement). The experimental data collection parameters for both measurements are summarized in Table I.

IV. RESULTS

A. GS

The refinement of GS is straightforward and yields agreement factors of $R=0.0367$, $S=3.15$ and $R=0.0509$, $S=3.65$ for the TriCS and D9 dataset, respectively. The results are in agreement with earlier refinements of the GS structure based on x-ray¹⁷ and neutron¹⁶ measurements. For details on the refined structural parameters see EPAPS Tables I and II.²⁸ The occupation o of the two different deuterium positions is refined independently, resulting in almost equal values of $o[D1]=0.47(1)$ and $o[D2]=0.50(1)$ for the TriCS dataset. For the D9 dataset, occupations of $o[D1]=0.35(1)$ and $o[D2]=0.36(1)$ are obtained, in agreement with the published data.¹⁷

B. GS+SI

The refinement of the structure of the mixed state GS + SI is not as straightforward. A naive refinement of the structure, as performed for GS leads to negative displacement parameters for the atoms Fe and O1 of the $[\text{Fe}(\text{CN})_5\text{NO}]$ molecule, showing that the main changes concomitant with the excitation of the metastable state SI occur at the Fe-N-O group, as was already recognized by Rüdlinger *et al.*¹⁶ However, since we know the population of SI to be about 22% from the transmission measurement, one can refine more elaborate models and test especially the isonitrosyl configuration (Fe-O-N) suggested by Carducci *et al.*¹⁷

1. Model with two oxygen positions

Introducing two positions for the oxygen atom of the $[\text{Fe}(\text{CN})_5\text{NO}]$ molecule, O1 and O1a (weighted with the population of GS and SI, respectively), the refinement converges to $R=0.0437$, $S=3.83$ and $R=0.0518$, $S=3.35$ for the TriCS and D9 dataset, respectively. The displacement parameters of the two oxygen atoms have to be chosen isotropic in order to obtain a clean refinement. Introducing anisotropic displacement parameters on these positions leads to unphysical (negative) values, because the thermal ellipsoids of the two atoms overlap. Since the occupation of the two positions is not equal, the scattering density distribution in this region is not uniform. Therefore the refinement of two thermal ellipsoids can easily lead to unphysical solutions, describing the observed scattering density as well as the one with two atoms having isotropic displacement parameters (spheres). This was actually done in Ref. 16 by averaging two spheres of different radii and different origins by one ellipsoid (with negative values of the displacement parameters of O1). The details on the structural parameters are given in EPAPS Tables III and IV.²⁸ The equivalent displacement parameters U_{eq} ²⁹ are indicated in order to ease the comparison between the anisotropic displacement parameters of

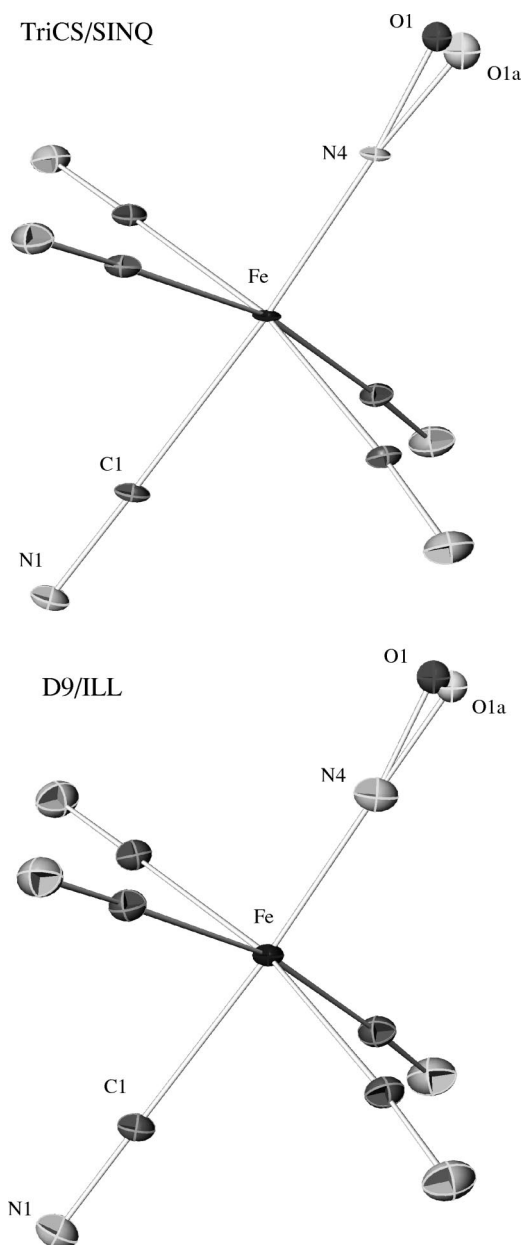


FIG. 6. View of the $[\text{Fe}(\text{CN})_5\text{NO}]$ molecule along the c axis (10° inclined) of the crystal in the model with two oxygen positions for O1. The two oxygen positions of the GS and SI are indicated on the same molecule. The upper picture shows the result from the refinement of the TriCS dataset and the lower picture that from the D9 dataset.

the other atoms [see EPAPS Table III (Ref. 28)] with those of the two oxygen atoms. Figure 6 shows the $[\text{Fe}(\text{CN})_5\text{NO}]$ molecule with the thermal ellipsoids and spheres as determined in the refinement. The two different oxygen positions O1 and O1a of GS and SI are drawn on the same molecule in order to ease the direct comparison between the two states GS and SI.

A stringent test of the stability of the refinement is obtained when refining the occupancy $o[\text{O1a}]$ of the oxygen atom O1a (excited state SI) with the restriction that the sum of the two occupancies ($o[\text{O1}] + o[\text{O1a}]$) is always the full

TABLE II. Distances and angles in GS and GS/SI of SNP.

	TriCS				D9			
	GS	GS+SI ^a	GS+SI ^b	GS+SI ^c	GS	GS+SI ^a	GS+SI ^b	GS+SI ^c
N4-O1	1.133(3)	1.128(6)	1.134(8)	1.133	1.129(4)	1.149(12)	1.156(14)	1.129
N4-O1a		1.15(2)				1.142(10)		
N4a-O1a			1.10(3)	1.13(2)			1.122(18)	1.150(7)
Fe-N4	1.674(2)	1.668(2)	1.660(6)	1.674	1.680(3)	1.699(2)	1.683(11)	1.680
Fe-N4a			1.71(2)				1.724(13)	
Fea-N4a				1.69(1)				1.716(6)
Fe-O1	2.806(3)	2.729(6)	2.793(6)	2.806	2.808(4)	2.834(10)	2.837(10)	2.808
Fe-O1a		2.81(2)		2.81(2)		2.848(12)	2.844(12)	
Fea-O1a				2.81(2)				2.863(6)
Fe-C1	1.927(3)	1.922(3)	1.921(3)	1.927	1.926(3)	1.921(3)	1.920(3)	1.926
Fea-C1a				1.942(16)				1.903(6)
Fe-C2	1.934(2)	1.929(2)	1.928(2)	1.934	1.937(2)	1.937(2)	1.938(2)	1.937
Fe-C3	1.947(2)	1.940(2)	1.938(2)	1.947	1.946(2)	1.948(2)	1.948(2)	1.946
C1-N1	1.165(3)	1.165(3)	1.164(3)	1.165	1.168(4)	1.169(3)	1.168(3)	1.168
C2-N2	1.163(2)	1.161(2)	1.161(2)	1.163	1.163(3)	1.167(2)	1.167(2)	1.163
C3-N3	1.163(2)	1.160(2)	1.163(2)	1.163	1.163(3)	1.166(2)	1.163(2)	1.163
Fe-N4-O1	1.37(8)	2.45(15)	1.6(2)	1.37	1.43(11)	3.2(2)	1.8(4)	1.43
Fe-N4-O1a		2.5(5)				0.4(2)		
Fe-N4a-O1a			1.1(9)				1.5(5)	
Fea-N4a-O1a				1.7(4)				1.95(19)
C1-Fe-N4	176.70(13)	176.63(14)	175.7(2)	176.70	176.24(16)	176.51(13)	175.1(3)	176.24
C1-Fe-N4a			179.2(8)				178.4(4)	
C1a-Fea-N4a				176.7(7)				177.2(3)
C2-Fe-N4	93.25(8)	93.30(9)	92.66(16)	93.25	93.01(10)	92.93(9)	91.9(2)	93.01
C3-Fe-N4	97.63(8)	97.67(9)	98.25(16)	97.63	97.80(11)	97.23(9)	98.1(2)	97.80
C3-Fe-C1	84.66(8)	84.67(9)	84.70(9)	84.66	84.82(11)	85.20(9)	85.24(9)	84.82
C3-Fe-C2	169.08(11)	168.98(12)	169.03(12)	169.08	169.14(14)	169.80(11)	169.88(11)	169.14
C3-Fe-C2'	88.22(7)	88.20(7)	88.24(8)	88.22	88.44(8)	88.55(7)	88.48(7)	88.44
C3-Fe-C3'	91.19(9)	91.33(10)	91.25(10)	91.19	91.20(12)	91.05(9)	91.06(9)	91.20
Fe-C1-N1	179.3(2)	179.3(2)	179.4(2)	179.3	179.9(3)	179.7(2)	179.7(2)	179.9
Fe-C2-N2	178.47(14)	178.43(15)	178.37(16)	178.47	177.94(18)	178.31(14)	178.43(15)	177.94
Fe-C3-N3	176.24(15)	176.38(16)	176.26(16)	176.24(15)	176.38(18)	176.17(15)	176.17(15)	176.38

^aModel with two oxygen positions.

^bModel with two NO ligands.

^cModel with two $[\text{Fe}(\text{CN})_5\text{NO}]$ molecules and GS fixed.

occupation of the site. The refinement converges to 22% occupation for SI, as determined independently from the transmission measurement for the TriCS dataset, and to 44% occupation for SI for the D9 dataset with the same structural parameters as obtained with fixed occupation.³⁰

The main changes between GS and SI occur at the Fe-N4-O1/O1a angle (Table II) while the N4-O1 distance in both configurations remains the same within standard deviations. The structural parameters obtained for Fe, N4, O1, and O1a agree for the two datasets. The displacement parameters show some deviations, especially the parameters U_{11} of Fe and N4. This may be explained by the larger dataset for the D9 data, covering more reflections at higher $\sin \theta/\lambda$ values, which are highly sensitive to the displacement parameters. Compared to the pure GS the Fe-N4-O1 angle of GS+SI is increased from 1.37° to 2.44° in the TriCS refinement and from 1.43° to 3.2° in the D9 refinement. One finds a rather

small value $U_{11}=0.4 \times 10^{-3} \text{ \AA}^2$ of Fe in the refinement of the TriCS dataset. This is a consequence of the smaller $\sin \theta/\lambda$ range in the TriCS datasets. In principle, refining the anisotropic displacement parameters of one Fe atom at a position, where in reality two Fe atoms are located at two slightly different positions, should lead to larger values of U_{11} due to the disorder at this position.

2. Model with two NO ligands

Introducing two NO ligands N4-O1 and N4a-O1a, i.e., two positions for oxygen and nitrogen, the two datasets can be refined almost equally well as in the two-oxygen-position model. Agreement factors of $R=0.0459$, $S=4.01$ and $R=0.0525$, $S=3.35$ are obtained for the TriCS and D9 dataset, respectively. In the TriCS dataset the displacement parameters for Fe, N4, N4a, O1, and O1a have to be chosen

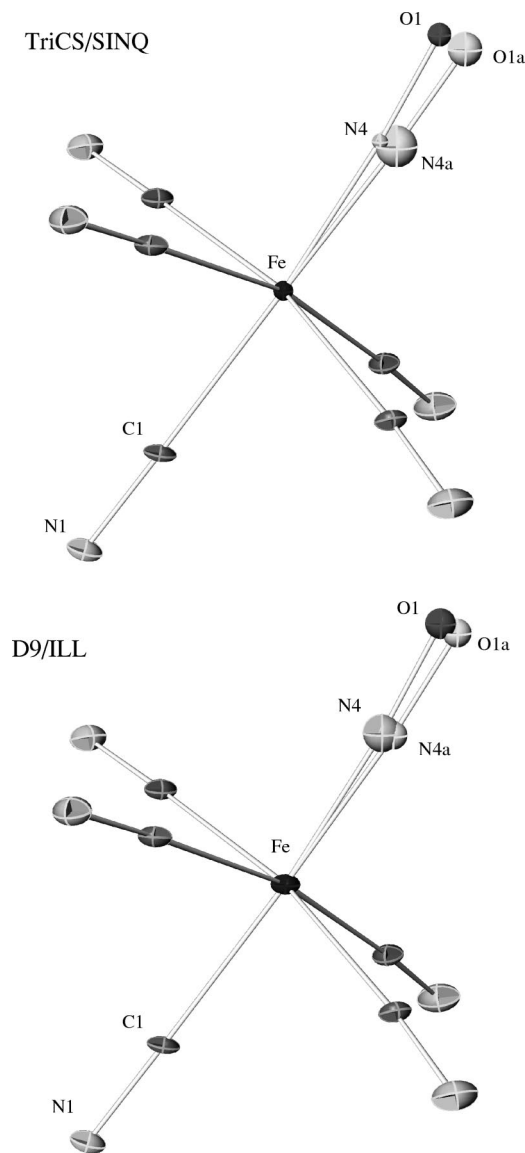


FIG. 7. View of the $\text{Fe}[(\text{CN})_5\text{NO}]$ molecule along the c axis of the crystal (10° inclined) in the model with two NO ligands. The two NO ligands of the GS (N4-O1) and SI (N4a-O1a) are indicated on the same molecule. The upper picture shows the result from the refinement of the TriCS dataset and the lower picture that from the D9 dataset.

isotropic. In the D9 dataset $U_{ij}[\text{Fe}]$ can be chosen anisotropic. The details on the refined parameters are given in EPAPS Tables V and VI.²⁸

The main changes between GS and SI in this model occur at the C1-Fe-N4 bond (see Table II). The Fe-N4 (GS) distance is increased from $1.674(2)$ Å to $1.71(2)$ Å ($\Delta = 0.036$ Å) in Fe-N4a (SI) for the TriCS dataset and from $1.680(3)$ Å to $1.724(13)$ Å ($\Delta = 0.044$ Å) in the D9 dataset. The C1-Fe-N4 angle is $179.2(8)^\circ$ (TriCS) and $178.4(4)^\circ$ (D9) in SI (C1-Fe-N4a) whereas for GS it is $176.70(13)^\circ$ (TriCS) and $176.24(16)^\circ$ (D9). The N4-O1 (N4a-O1a) distance and the Fe-N4-O1 (Fe-N4a-O1a) angle remain practically unchanged. In the TriCS refinement the isotropic displacement parameters U_{iso} of N4 and O1 are rather small

when compared to those of N4a and O1a. This is again a consequence of refining the displacement parameters of two atoms at almost identical positions. Figure 7 illustrates the result that for SI the quasifourfold axis of the molecule is nearly in a linear configuration, whereas the GS shows a slight bending away from the fourfold axis. The refinement with two NO ligands has the advantage that the GS configuration remains unaltered when compared to the pure ground state, whereas in the two-oxygen-position model the Fe-N4 angle was changed. The fact that these two models lead to similar agreement factors in the refinement is not completely astonishing, since already in 1979 Feltham and Enemark³¹ concluded from an extensive study of different nitrosyl compounds: The various positions for the oxygen atoms of the disordered bent nitrosyl ligand can usually be determined but the coordinates of the nitrogen atoms are often impossible to define uniquely.

3. Model with one NO and one inverted NO ligand

Can the data also be explained with the isonitrosyl configuration ON of the NO ligand of SI, as proposed by Carlucci *et al.*¹⁷?

Introducing for the metastable state SI an inverted NO ligand, i.e., besides the N4-O1 for the GS a ligand O1a-N4a is used in the refinement, no stable refinement yielding physically meaningful parameters can be achieved. Either the outer atom N4a has displacement parameters which are more than one order of magnitude higher than the others ($U_{\text{iso}} = 0.13$ Å² corresponding to a mean displacement of $\langle u_j \rangle = 0.36$ Å) or the inner atom O1a has negative displacement parameters, when constraining $U_{\text{iso}}[\text{N4a}]$ to $U_{\text{iso}}[\text{O1}]$. This result is independent of whether the displacement parameters are chosen isotropic or anisotropic. The reason for this behavior becomes evident when looking at the contributions to the nuclear structure factor F_{N} [see Eq. (4)]. Inserting a nitrogen atom for an oxygen atom on the outer position, the neutron-scattering length b_j is increased from 5.8 barn to 9.36 barn. If the observed structure factors do not agree with this model, the Debye-Waller factor $\exp[-W_j(\mathbf{Q})]$ must be reduced in the refinement. Therefore the displacement parameter U_{iso} is enhanced until the overestimated scattering density is reduced to the observed value. Forcing the values U_{iso} of the outer atoms O1 and N4a to reasonable values, the problem is handed over to the inner position, where the situation is inverted. Here the neutron-scattering length b_j is reduced from 9.36 barn to 5.8 barn when replacing N4 with O1a. Therefore U_{iso} is decreased until the missing scattering density is obtained, thereby yielding unphysical values of $U_{\text{iso}}[\text{O1a}]$.

Reducing the population of SI (i.e., the number of inverted configurations O1a-N4a) leads also to the reduction of the values for the structure factors. In other words, if the assumed population of SI is overestimated, the displacement parameters will correct for this wrong input in the refinement in the same manner as described above. To sort out this possibility as an explanation for the occurrence of negative displacement parameters, the occupation of N4a and O1a was systematically reduced and the refinements were repeated. It was found that the population of SI has to be reduced to

TABLE III. Isotropic mean-square displacement parameters U_{iso} (\AA^2) from refinement of SI with fixed GS.

	TriCS		D9		From Ref. 14	
	Nitrosyl	Isonitrosyl	Nitrosyl	Isonitrosyl	Nitrosyl	Isonitrosyl
P_{SI} (%)	22	22	44	44	37	37
R	0.058	0.058	0.051	0.052		
S	4.7	4.8	3.2	3.3		
$U_{iso}(N4a)$	0.004(1)	0.033(3)	0.020(1)	0.029(1)	0.0040(4)	0.0102(4)
$U_{iso}(O1a)$	0.004(2)	-0.019(3)	0.004(1)	-0.002(1)	0.0163(5)	0.0088(5)
No. of variables	64	64	64	64	55	55

values lower than 1% and 3% for the TriCS and D9 dataset to get rid of this problem. Furthermore the two possibilities to reduce the value of the structure factors F (reduction of occupation and decrease of the values of the displacement parameters) have a different \mathbf{Q} dependence. Therefore the influence of the two effects can be separated well enough in the refinement, especially in the D9 dataset, where more reflections have been measured in the range up to $\sin \theta/\lambda = 0.73 \text{ \AA}^{-1}$.

Refining the occupation of the isonitrosyl configuration of SI leads to a decrease of the occupation of N4a and O1a to zero with arbitrary structural parameters for these two atoms. In order to get a stable refinement in the Fe-O1a-N4a configuration the positions and displacement parameters of N4, O1, N4a, and O1a have to be fixed. Using the same occupancies as in the refinements without NO inversion, considerably inferior agreement factors of $R=0.055$, $S=4.8$ and $R=0.081$, $S=4.51$ for the TriCS and D9 dataset are obtained for this configuration.

4. Models with fixed GS configuration

Since we know from infrared spectroscopy³² that the vibrations of the GS do not change in the excited state GS+SI, we performed also a refinement where the coordinates and displacement parameters of the GS were fixed to the values obtained in the refinement of the pure GS. Therefore two Fe[(CN)₅NO] molecules are introduced in the asymmetric unit, one with the parameters and population of GS and one for SI. The D₂O molecule and the sodium atoms are refined unrestricted, but using only one position for them in the mixed state GS+SI, as they are not involved in the excitation mechanism and therefore their changes in position and displacement parameters can be neglected. The lattice parameters of the GS were taken for this kind of refinement, in order to account for the fact that the distances within the Fe[(CN)₅NO] molecule of the GS do not change (the same results are obtained when introducing a GS molecule, corrected for different lattice parameters, in the GS+SI lattice). It has been shown¹⁷ that the changes of the rigid GS molecule are indeed very small, when allowed for translation and rotation in the GS+SI lattice. Furthermore the displacement parameters of the cyano ligands in the SI molecule are set to the corresponding values of GS, since a refinement of those leads to strong correlations because the positions of these atoms almost coincide with the GS positions. For the Fea,

N4a, and O1a isotropic displacement parameters are introduced in SI. Therefore 64 free parameters are refined to the mixed state GS+SI (see Table III). Carducci *et al.*¹⁷ used 55 free parameters in their refinement, by refining only isotropic displacement parameters to the two hydrogen positions (i.e., 2 instead of 12 parameters) and fixing the isotropic displacement parameter of Fe to its ground-state value.

The results of these refinements agree qualitatively with those obtained in the above explained refinements. Using the nitrosyl configuration (N bound) for SI one obtains stable refinement with quite reasonable displacement parameters for Fea, N4a, and O1a (see Table III) for both datasets (TriCS and D9). For the isonitrosyl configuration (O bound) on the other hand one obtains again negative displacement parameters for the inner atom O1a and rather large values for the outer atom N4a. The R values obtained for the two different refinements are almost equal (see Table III), therefore one has to apply other arguments in order to decide between the two models. The same situation was found in the x-ray refinements,¹⁷ which led those authors to the conclusion that the isonitrosyl configuration is the correct solution mainly due to stability arguments. We suggest that the nitrosyl configuration is the correct structural solution for SI since in the isonitrosyl configuration we obtain negative displacement parameters, which is unphysical. Furthermore the refinements in the nitrosyl configuration are stable when refining the population P_{SI} of SI, whereas those in the isonitrosyl configuration are not. For the D9 dataset one can find a refinement in the isonitrosyl configuration with reasonable displacement parameters for N4a and O1a when fixing the population of SI at $P_{SI} \sim 20\%$, in contradiction to the results shown in Fig. 5. This is not possible for the TriCS dataset, where the population P_{SI} is reduced to nearly zero. This reduction shows again the necessity of a separate detection of the population P_{SI} . Consequently, we can only vary the displacement parameters or the fractional coordinates in our refinements. The additional knowledge of the neutron-scattering lengths b_j of N and O opens the possibility of investigating the changes of the fractional coordinates and the displacement parameters when exchanging N and O.

5. Photodifference maps

Evidence for the isonitrosyl configuration in the x-ray experiments was also found when looking at photodifference maps,¹⁷ which are weighted differences between the struc-

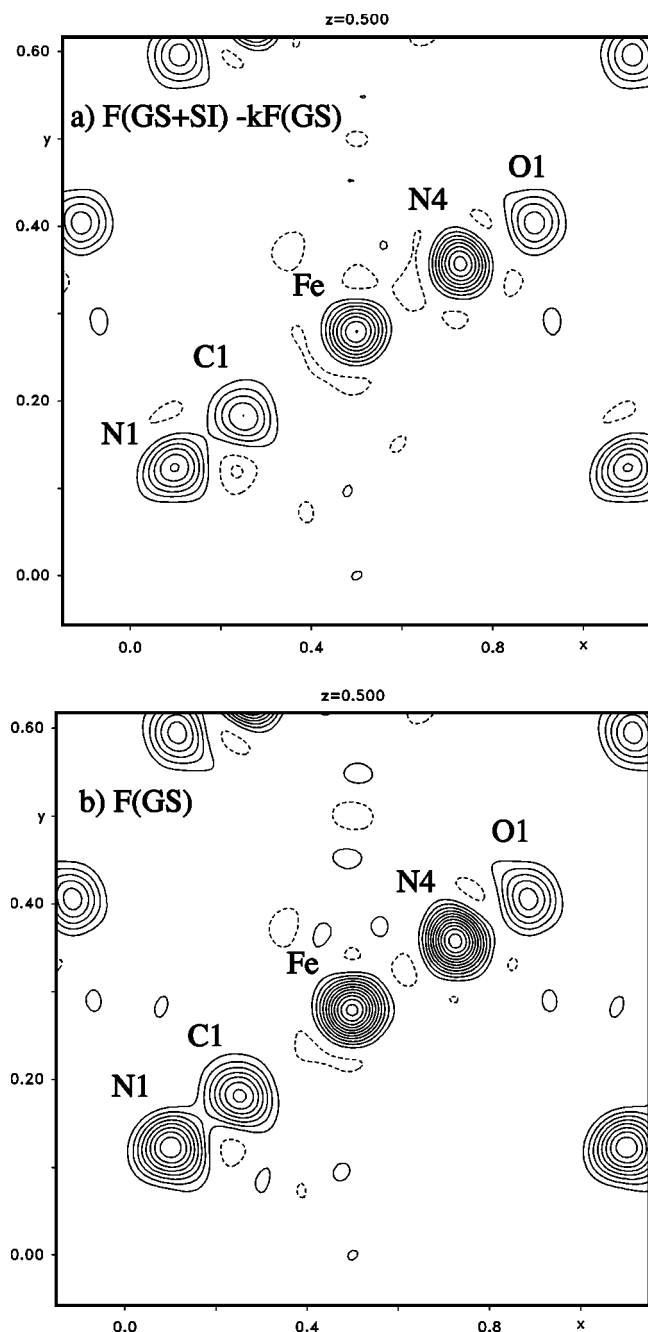


FIG. 8. (a) Photodifference map $F(\text{GS} + \text{SI}) - kF(\text{GS})$ for the TriCS datasets, i.e., $k=0.78$; contours $2 \text{ barn } \text{Å}^{-3}$. (b) Observed density in the TriCS measurement for the ground state; $F(\text{GS})$; contours $5 \text{ barn } \text{Å}^{-3}$.

ture factors of GS+SI and GS. Figure 8(a) shows the photodifference map $F(\text{GS} + \text{SI}) - kF(\text{GS})$ for the TriCS dataset in the plane $z=0.5$ (containing the N1-C1-Fe-N4-O1 axis) with the weighting factor $k=0.78$ for $F(\text{GS})$, since the transmission measurement yielded a population of 22% for SI. One finds a density of $17 \text{ barn } \text{Å}^{-3}$ at the N4 position compared to $9.17 \text{ barn } \text{Å}^{-3}$ at the O1 position. For direct comparison Fig. 8(b) illustrates the observed density in the GS, where a density of $58 \text{ barn } \text{Å}^{-3}$ was found at the N4 position compared to a density of $28 \text{ barn } \text{Å}^{-3}$ at the O1

position. Similar maps with a higher scattering density at the N4 position compared to the O1 position were found for the D9 dataset, confirming the results and interpretation of our least-square refinements.

V. CONCLUSIONS

The structural refinement of the neutron-diffraction data shows that a small change in the Fe-N4 bond length ($\approx 0.05 \text{ Å}$) and in the C1-Fe-N4 angle ($\approx 3.5^\circ$) are the only significant rearrangements in the nuclear structure connected with the excitation of the metastable state SI. This result is consistently found for two datasets with different population of the metastable state SI (22% and 44%). The elongation of the Fe-N4 bond length by about 0.05 Å was already found in the x-ray experiments of Pressprich *et al.*¹⁸ Also Carducci *et al.*¹⁷ could interpret their x-ray data in this manner with the same agreement factors as for the interpretation with the isonitrosyl configuration. The structural results for SI are therefore consistent for the two methods. The attempts to interpret the data using the isonitrosyl configuration for SI, as suggested by Carducci *et al.*,¹⁷ failed for the neutron data. The refinement does not converge to physically meaningful parameters. Neutron diffraction is the key technique to investigate a possible inversion of the nitrosyl-ligand since it allows easy distinction between N and O due to their sufficiently differing scattering lengths (9.36 barn versus 5.8 barn). This is reflected in the fact that those refinements, which were performed in the same manner as the x-ray refinements,¹⁷ yielded unphysical displacement parameters for the NO group in the isonitrosyl configuration or resulted in a strong reduction of the population P_{SI} . The isonitrosyl configuration can only be refined when constraining all displacement parameters of SI to those of GS. As soon as one of them is released, its refinement yields unphysical values. This elucidates the delicate problems which occur when constraints between the parameters of SI and GS are introduced in the refinement of the mixed state GS+SI. This is the reason why we prefer the structural refinements of the mixed state with no constraints on the GS, even when this results in small changes of the known GS structure. However, as already pointed out by Güdel,³³ a small structural change is not able to explain the extremely long lifetime ($> 10^7 \text{ s}$ at low temperatures) of the metastable state SI.

There are further experimental investigations which do not yield an unambiguous proof of the isonitrosyl configuration. It has been shown by electron paramagnetic resonance (EPR) measurements³⁴ that irradiation of SNP with x-rays (MoK_α) produces paramagnetic $[\text{Fe}(\text{CN})_5\text{NO}]^{3-}$ species in the crystal, which can also be excited into SI by irradiation with light. A clear ^{14}N hyperfine splitting is found, which demonstrates the existence of the Fe-N bond in SI for this $3d^7$ system. Further, an extended x-ray absorption fine structure analysis of irradiated CpNiNO received an elongation of the Ni-N and N-O bond lengths with respect to the ground state.³⁵ However, subsequent structure analysis by x-ray confirmed the isonitrosyl Ni-O-N configuration.³⁶ In a recent structure analysis of the compound $\text{Na}_2[\text{Ru}(\text{NO}_2)_4\text{OHNO}]2\text{H}_2\text{O}$ using synchrotron radiation,³⁷

the metastable state SI is described with a significant increase of the Ru-NO bond length and a decrease of the Ru-N-O angle. The attempt to refine SI with an isonitrosyl configuration (Ru-O-N) failed for this compound. On the other hand, the isostructural compound $K_2[Ru(NO_2)_4OHNO]2H_2O$ is refined in SI with the isonitrosyl configuration by Fomitchev and Coppens.³⁸ Strong evidence for the existence of the isonitrosyl structure is given by the DFT calculations.^{10,19,39} A stable energetic minimum is found for the isonitrosyl geometry, yielding an increase of the electric-field gradient at the Fe nucleus, an increase of the isomer shift, a significant frequency downshift of the vibrations and a higher energetic position of SI with respect to GS. The quantitative agreement between observed and calculated values is not very good, but qualitatively the calculations agree with the observations as they predict the changes in the correct direction. However, the DFT calculations cannot unambiguously show whether the calculated minimum in energy is occupied in reality when irradiating with light, since in all DFT calculations the isonitrosyl structure is introduced and the consequences for the physical parameters are calculated starting from this configuration. The same problematic situation exists for the interpretation of the results received by inelastic nuclear scattering.⁴⁰ The detected shifts of the stretching vibrations and deformation modes are known from IR/Raman spectroscopy.^{4,32,41} The interpretation of these shifts using DFT calculations is again based on the assumption that the isonitrosyl structure is established and subsequently the calculated vibrations are compared to the observed ones. A much stronger evidence is presented by isotopic substitution of Fe, N, and O in IR/Raman measurements.^{42,43} Here, the isotopes are fingerprints for the determination of the shift of the $\nu(\text{Fe-N})$ or $\nu(\text{Fe-O})$ stretching vibrations and $\delta(\text{Fe-N-O})$ or $\delta(\text{Fe-O-N})$ deformation modes. Unfortunately the shifts between the ^{14}N , ^{15}N , ^{16}O , and ^{18}O are quite small. They are decreasing between 0 cm^{-1} and 4 cm^{-1} . Consequently DFT or force field calculations were performed to estimate the amount of the shift. From this calculations it is predicted that the isonitrosyl configuration can explain the small decrease of 4 cm^{-1} for the $\delta(\text{Fe-}^{18}\text{O-}^{15}\text{N})$ deformation mode, which is of course in clear contradiction to our structure analysis.

Taking into account the results of recent absorption measurements we can present a detailed two-step process for the

population of the metastable state SI and a change of the electron density. Irradiation with blue-green light excites an electron into the antibonding $\pi^*(\text{NO})$ orbital with a lifetime in the $\pi^*(\text{NO})$ orbital of several μs :²⁰ $\text{Fe}(3d_{xz,yz};3d_{xy}) \rightarrow \pi^*(\text{NO}) \rightarrow \text{SI}$. This lifetime is long enough for the remaining electrons (mainly at the Fe) to relax into a new configuration. The excited electron relaxes from the $\pi^*(\text{NO})$ orbital back into the $3d(\text{Fe})$ orbitals embedded in this new potential. From the measured shift in the quadrupole splitting and from the change of the isomer shift observed by Mössbauer measurements,⁴⁴ it was concluded that not the whole excited charge is relaxing back to the $3d(\text{Fe})$ orbitals, but a small amount remains in the $\pi^*(\text{NO})$. While thereby the population of the $\pi^*(\text{NO})$ orbital is increased, those of the $3d_{z^2}$, $3d_{xz,yz}$, and $4p_z$ are decreased. This redistribution of charge density might also explain why the observed transitions in the absorption measurements do not agree very well with the energetic position from the calculated orbital configuration, which is based on the isonitrosyl configuration. On the other hand it also could lead to misinterpretation of x-ray data, where the scattering occurs at the electrons.

The conclusion of a small change in the Fe-N-O angle fits also in the classification scheme of Feltham and Enemark,³¹ where the nitrosyl complexes are classified as $[M(\text{NO})_m]^n$ species with n being the total number of electrons associated with the metal d and/or $\pi^*(\text{NO})$ orbitals. Their final conclusion is that for six-coordinate mononitrosyl complexes the M-N-O angle is $180 \pm 10^\circ$ for $n \leq 6$ (SNP), $145 \pm 10^\circ$ for $n = 7$, and $125 \pm 10^\circ$ for $n = 8$. Moreover the almost linear configuration of the C1-Fe-N4 angle in SI compared to GS is in agreement with Mössbauer experiments, where an increase of this angle towards a more linear configuration was observed.⁴⁵

ACKNOWLEDGMENTS

This work was partially performed at the SINQ, Paul Scherrer Institut, Villigen, Switzerland. Financial support by the Swiss National Science Foundation (Grant No. 21-57084.99), the Deutsche Forschungsgemeinschaft (Grant No. WO618/5-1), and the European Community (INTAS, Grant No. 2000-0651) is gratefully acknowledged. We are very indebted to N. K. Hansen and V. Petříček for helpful discussions.

*Electronic address: dominik.schaniel@uni-koeln.de; present address: Institut für Mineralogie, University at Cologne, D-50674 Köln, Germany.

¹M. Imlau, S. Haussühl, T. Woike, R. Schieder, V. Angelov, R. Rupp, and K. Schwarz, *Appl. Phys. B: Photophys. Laser Chem.* **68**, 877 (1999).

²T. Woike, S. Haussühl, B. Sugg, R. Rupp, J. Beckers, M. Imlau, and R. Schieder, *Appl. Phys. B: Photophys. Laser Chem.* **63**, 243 (1996).

³H. Zöllner, W. Krasser, T. Woike, and S. Haussühl, *Chem. Phys. Lett.* **161**, 497 (1989).

⁴T. Woike, H. Zöllner, W. Krasser, and S. Haussühl, *Solid State Commun.* **73**, 149 (1990).

⁵T. Woike and S. Haussühl, *Solid State Commun.* **86**, 333 (1993).

⁶K. Ookubo, Y. Morioka, H. Tomizawa, and E. Miki, *J. Mol. Struct.* **379**, 241 (1996).

⁷P. Coppens, D.V. Fomitchev, M.D. Carducci, and K. Culp, *J. Chem. Soc. Dalton Trans.* **6**, 865 (1998).

⁸D. Fomitchev, I. Novozhilova, and P. Coppens, *Tetrahedron* **56**, 6813 (2000).

⁹P. Gütllich, Y. Garcia, and T. Woike, *Coord. Chem. Rev.* **219-221**, 839 (2001).

¹⁰P. Coppens, I. Novozhilova, and A. Kovalevsky, *Chem. Rev. (Washington, D.C.)* **102**, 861 (2002).

¹¹H. Zöllner, T. Woike, W. Krasser, and S. Haussühl, *Z. Kristallogr.* **188**, 139 (1989).

- ¹²T. Woike, W. Krasser, H. Zöllner, W. Kirchner, and S. Haussühl, *Z. Phys. D: At., Mol. Clusters* **25**, 351 (1993).
- ¹³J. Schefer, T. Woike, M. Imlau, and B. Delley, *Eur. Phys. J. B* **3**, 349 (1998).
- ¹⁴P. Manoharan and W. Hamilton, *Inorg. Chem.* **2**, 1043 (1963).
- ¹⁵F. Bottomley and P. White, *Acta Crystallogr., Sect. B: Struct. Crystallogr. Cryst. Chem.* **35**, 2193 (1979).
- ¹⁶M. Rüdlinger, J. Schefer, G. Chevrier, N. Furer, H. Güdel, H. Haussühl, and G. Heger, *Z. Phys. B: Condens. Matter* **83**, 125 (1991).
- ¹⁷M. Carducci, M. Pressprich, and P. Coppens, *J. Am. Chem. Soc.* **119**, 2669 (1997).
- ¹⁸M.R. Pressprich, M.A. White, Y. Vekhter, and P. Coppens, *J. Am. Chem. Soc.* **116**, 5233 (1994).
- ¹⁹B. Delley, J. Schefer, and T. Woike, *J. Chem. Phys.* **107**, 10 067 (1997).
- ²⁰D. Schaniel, J. Schefer, B. Delley, M. Imlau, and T. Woike, *Phys. Rev. B* **66**, 085103 (2002).
- ²¹J. Schefer, M. Könnecke, A. Murasik, A. Czopnik, T. Strässle, P. Keller, and N. Schlumpf, *Physica B* **276-278**, 168 (2000).
- ²²P. Allenspach, *Neutron News* **11**, 15 (2000).
- ²³V. Petříček and M. Dušek, *The Crystallographic Computing System JANA2000* (Institute of Physics, Praha, 2000).
- ²⁴W. Barrett and W. Wallace, *J. Am. Chem. Soc.* **76**, 366 (1954).
- ²⁵P.J. Becker and P. Coppens, *Acta Crystallogr., Sect. A: Cryst. Phys., Diffr., Theor. Gen. Crystallogr.* **30**, 129 (1974).
- ²⁶J.-O. Lundgren, Institute of Chemistry, University of Uppsala, Report No. UUIC B13-4-05, 1982 (unpublished).
- ²⁷V. Sears, *Neutron News* **3**, 26 (1992).
- ²⁸See EPAPS Document No. E-PRBMDO-68-072334 for details on refined structural parameters. A direct link to this document may be found in the online article HTML reference section. The document may also be reached via the EPAPS homepage (<http://www.aip.org/pubservs/epaps.html>) or from <ftp.aip.org> in the directory /epaps/. See the EPAPS homepage for more information.
- ²⁹ $U_{eq} = \sum_{i,j} U_{ij} b_i b_j a_i a_j$ where $\mathbf{b}_1, \mathbf{b}_2, \mathbf{b}_3$ and $\mathbf{a}_1, \mathbf{a}_2, \mathbf{a}_3$ are the reciprocal and direct lattice vectors, respectively.
- ³⁰45% population of SI was assumed by Rüdlinger *et al.* (Ref. 16) for the refinement of the D9 data.
- ³¹R. Feltham and J. Enemark, in *Topics in Inorganic and Organometallic Stereochemistry*, edited by G. Geoffroy (Wiley, New York, 1981), pp. 155–215.
- ³²J. Guida, P. Aymonino, O. Piro, and E. Castellano, *Spectrochim. Acta, Part A* **49**, 535 (1993).
- ³³H. Güdel, *Chem. Phys. Lett.* **175**, 262 (1990).
- ³⁴C. Terrile, O. Nascimento, I. Moraes, E. Castellano, O. Piro, J. Guida, and P. Aymonino, *Solid State Commun.* **73**, 481 (1990).
- ³⁵L. Chen, M. Bowman, Z. Wang, P. Montano, and J. Norris, *J. Phys. Chem.* **98**, 9457 (1994).
- ³⁶D. Fomitchev, T. Furlani, and P. Coppens, *Inorg. Chem.* **37**, 1519 (1998).
- ³⁷A. Puig-Mollina, H. Müller, A.-M. Le Quéré, G. Vaughan, H. Graafsma, and A. Kvik, *Z. Anorg. Allg. Chem.* **626**, 2379 (2000).
- ³⁸D. Fomitchev and P. Coppens, *Inorg. Chem.* **35**, 7021 (1996).
- ³⁹P. Boulet, M. Buchs, H. Chermette, C. Daul, E. Furet, F. Gilar-doni, F. Rogemond, C. Schläpfer, and J. Weber, *J. Phys. Chem. A* **105**, 8991 (2001).
- ⁴⁰H. Paulsen, V. Rusanov, R. Benda, C. Herta, V. Schünemann, C. Janiak, T. Dorn, A. Chumakov, H. Winkler, and A. Trautwein, *J. Am. Chem. Soc.* **124**, 3007 (2002).
- ⁴¹Y. Morioka, *Spectrochim. Acta, Part A* **50**, 1499 (1994).
- ⁴²Y. Morioka, S. Takeda, H. Tomizawa, and E. Miki, *Chem. Phys. Lett.* **292**, 625 (1998).
- ⁴³M. Chacon-Villalba, J. Guida, E. Varetto, and P. Aymonino, *Spectrochim. Acta, Part A* **57**, 367 (2001).
- ⁴⁴T. Woike, W. Kirchner, K. Hyung-sang, S. Haussühl, V. Rusanov, V. Angelov, S. Ormandjiev, T. Bochev, and A. Schroeder, *Hyperfine Interact.* **77**, 265 (1993).
- ⁴⁵T. Woike, M. Imlau, V. Angelov, J. Schefer, and B. Delley, *Phys. Rev. B* **61**, 12 249 (2000).